

# Electric characteristics of very small Normal-Mode Helical Antenna in Human Body Conditions

Dang Tien Dung, Nguyen Quoc Dinh  
Le Quy Don Technical University  
Hanoi, Vietnam  
Email:dangtiendung@tcu.edu.vn  
dinhnq@mta.edu.vn

Naobumi Michishita  
National Defense Academy  
Yokosuka, Japan  
Email:naobumi@nda.ac.jp

Yoshihide Yamada  
Universiti Teknologi Malaysia  
Kuala Lumpur, Malaysia  
Email:ndayamada@yahoo.co.jp

Ha Quoc Anh  
Telecommunications University  
Khanhhoa, Vietnam  
Email:haquocanh1812@gmail.com

**Abstract**—Recently, very small radio wave sensors (RWS) are tried to be put in to a human body for human health care purpose. As for a very small antenna in a sensor, normal-mode helical antenna (NMHA) is suitable due to its high efficiency with very small sizes. In this paper, antenna design method and electrical characteristics are clarified for very small NMHA which size is from 0.03 to 0.06 wavelengths in a human body conditions. Firstly, antenna self-resonant structures are clarified through electromagnetic simulations. Next, antenna input resistance changes for human body conductivity changes are clarified. Moreover, radiated power changes are also examined.

**Index terms** - NMHA; RWS; Human Body; FEKO; MoM.

## I. INTRODUCTION

Human health care ingestible radio wave sensor has been researchs before. Therefore, there have been many recommendations and standards for use RWS of the countries in the world [1] [2] [3]. Similarly, in case of NMHA, many types of antennas have been studied to use in RWS. NMHA has the advantage of being very small size and high radiation efficiency. Therefore, NMHA can be fit into the small size of RWS. In this paper, very small NMHA, which is less than  $0.06 \lambda_g$  ( $0.03 \lambda_g \div 0.06 \lambda_g$ ) is examined. Important design specification such as antenna structure, antenna input resistance, radiated electric field distribution and antenna gain are obtained by FEKO 7.0 simulations [4]. Through this study, almost fundamental characteristics of very small size of NMHA less than  $0.06 \lambda_g$  are clarified [5] [6]. The conductivity and relative permittivity of the human body are two main parameters, which affect performance of NMHA.

## II. SIMULATION MODEL AND PARAMETERS

Simulation model of NMHA used in human's muscle is show in Fig.1. Simulation is carried out by commercial electromagnetic FEKO 7.0 simulator. NMHA is embedded inside a dielectric cylinder with dimensions of Length ( $L$ ) x Width ( $W$ ) 60 x 60 mm as practical human muscle using human tissues parameters at the frequency for implanted

medical device applications of 402 MHz [3].  $H$ ,  $D$ ,  $N$  indicate height, diameter of antenna and number of turns respectively.

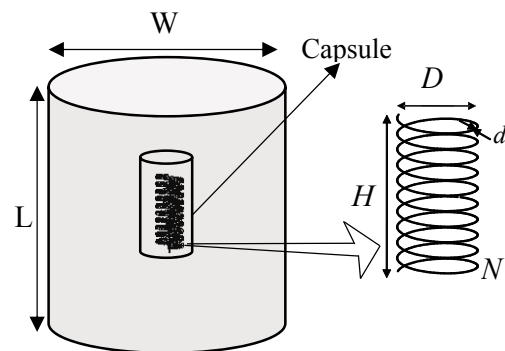


Fig. 1: Simulation model

TABLE I: SIZE OF NMHA STRUCTURE

Method	MoM
Frequency	402MHz
Dielectric Constant (Muscle)	$\epsilon_r = 53; \mu_r = 1; \sigma = 0; \rho = 0.89 (S/m); \rho = 1040 (kg/m^3)$
Mesh size of antenna wire	$\lambda_g/100$
Mesh size of material	$\lambda_g/40$
Number of turns	$N = 5; 7; 9$
Metallic wire	Copper ( $\sigma = 58 * 10^6 [1/\Omega m]$ )
Memory	1538 MB
Diameter of Antenna wire (d)	0.3; 0.4; 0.5 (mm)
Calculated time	2.267 h/sim

Simulation parameters of NMHA used in human body are shown in TABLE I. Diameter of antenna wire (d) is set to be sequently 0.3 mm, 0.4 mm and 0.5 mm. Antenna height ( $H$ ) and diameter ( $D$ ) need to be adjusted so as to NMHA achieves self resonance in various number of turns  $N = 5; 7;$

9. Metallic wire is defined as copper with conductivity  $\sigma = 58 * 10^6$  [1/  $\Omega$  m]. Dielectric constants are set to be equal to constants of practical human muscle with relative permittivity  $\epsilon_r = 53$ ; relative permeability  $\mu_r \approx 1$  and conductivity  $\sigma = 0.89$  (S/m). The results are compared to those with respect to  $\sigma = 0$ . Mesh size of antenna wire is set to be 1/100 wavelength in material ( $\lambda_g$ ); mesh sizes of material are set to be  $\lambda_g/40$  to investigate simulation accuracy. NMHA is put inside dielectric substrate with  $\epsilon_r = 53$ , therefore the wavelength in material ( $\lambda_g$ ) = 102 mm. Relation between wavelength in material ( $\lambda_g$ ) and wavelength in free space ( $\lambda_0$ ) is expressed as following:

$$\lambda_g = \frac{\lambda_0}{\sqrt{\epsilon_r \mu_r}} \quad (1)$$

### III. SELF RESONANT STRUCTURE

The input impedance of an antenna is expressed as following

$$Z_{in} = R_{in} + jX_L - jX_D \quad (2)$$

where,  $R_{in}$  denotes the input resistance of NMHA.  $X_L$  and  $X_D$  are the inductive reactance and capacitive reactance of loop antenna and dipole antenna [7]. A self-resonant condition of NMHA is given by  $X_L = X_D$ . From self-resonant condition, self-resonant structure of NMHA in human body will be determined as shown in Fig. 2. The self-resonant structure of the NMHA is less than  $0.05 \lambda_g$  which are obtained the similar way in the our published results [8] [9]. The NMHA structure result is obtained by using the smallest dimension is  $0.03 \lambda_g$ . Some structures cannot be examined because the height of the NMHA is very small. Hence, the wire loop may overlap to each other.

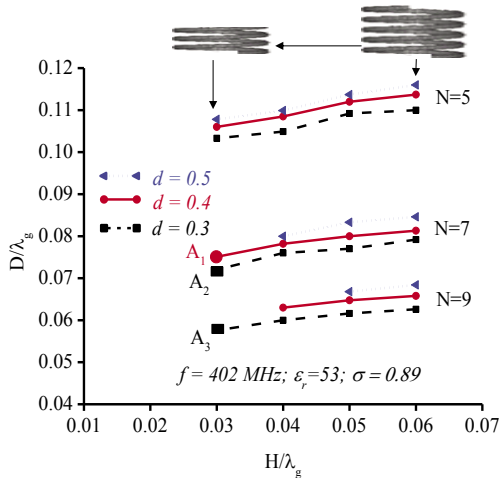


Fig. 2: Self-Resonant Structures

To ensure simulation, antenna performance of structure  $A_1$ ,  $A_2$ ,  $A_3$  in Fig. 2 are investigated to clarify at the next section. Size of structure  $A_1$ ,  $A_2$ ,  $A_3$  is shown in TABLE II.

TABLE II: SIZE OF NMHA STRUCTURES

N = 7		N = 9
d = 0.3	d = 0.4	d = 0.3
$A_1$ (H x D mm)	$A_2$ (H x D mm)	$A_3$ (H x D mm)
3.08 x 7.42	3.08 x 7.73	3.08 x 5.9

### IV. ELECTRIC FIELD DISTRIBUTION

The near field distribution of the  $A_2$  structure is shown in Fig. 3 and Fig. 4, where the two dimensions of material are 10 mm and 60 mm, respectively. As can be seen in the Fig. 3, in region close to the antenna, the radiations are the same in two cases  $\sigma = 0$  S/m and  $\sigma = 0.89$  S/m. However, there is a rapid reduction of the radiation field at the distance of about 10 mm in the case  $\sigma = 0.89$  S/m. In the case  $\sigma = 0$  S/m, the decrease of radiation field is not significant. The reduced radiation field is clearer, as shown in Fig. 4. The effect of material having larger conductivity is very high on the radiation. In other words, the human body absorbs electromagnetic waves. Loss of propagation in human body needs to be determined.

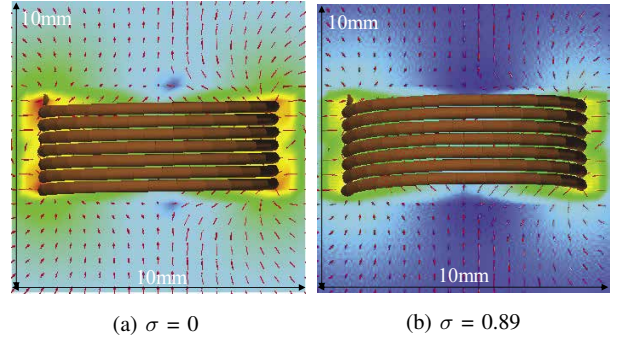


Fig. 3: Near area

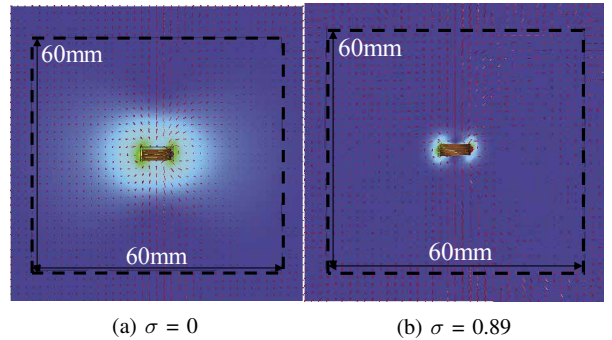


Fig. 4: Wide area

### V. INPUT RESISTANCE

Input resistance of NMHA in human body condition can be calculated as following

$$R_{in} = R_{ant} + R_{abs}, \quad (3)$$

where,  $R_{in}$  indicates the input impedance of NMHA in human body;  $R_{ant}$  is the resistance of antenna itself involving radiated resistances of antenna and  $R_{abs}$  is the absorbing resistance by human tissues. The resistance of antenna itself is expressed by the following equation.

$$R_{ant} = R_{rL} + R_{rD} + R_{\Omega}, \quad (4)$$

where,  $R_{rD}$  and  $R_{rL}$  express radiation resistances of NMHA.  $R_{\Omega}$  is ohmic resistance of antenna wire. Calculated results of input resistance  $R_{in}$  by an electromagnetic FEKO 7.0 simulator are shown in Fig. 5. The input resistance of the NMHA with the size less than  $0.05 \lambda_g$  are obtained the changing of results similar size larger than  $0.05 \lambda_g$ . The bandwidth characteristics of three structures  $A_1$ ,  $A_2$ ,  $A_3$  are shown in Fig. 6. In this case, the simulation results show that the antenna achieves very good bandwidth at voltage standing wave ratio (VSWR) = 2. The fractional bandwidths of  $A_1$ ,  $A_2$ ,  $A_3$  are about 2.16 %, 1.87 % and 1.88 %, respectively.

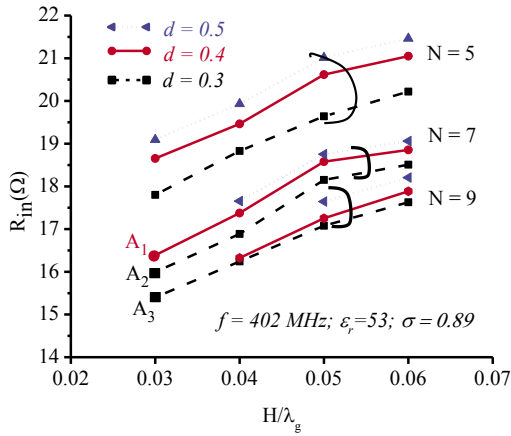


Fig. 5: Input Resistance

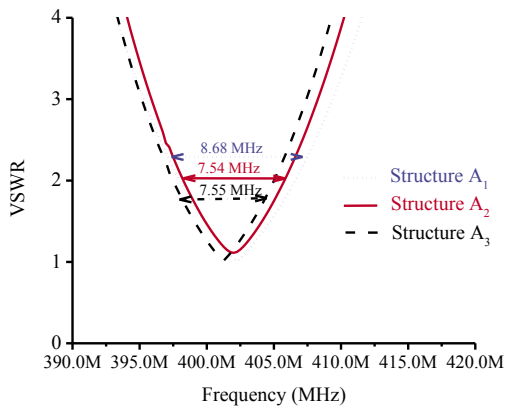


Fig. 6: VSWR characteristics

The input resistance  $R_{in}$  of  $A_2$  structure depends on conductivity of material are shown in Fig. 7.  $R_{in}$  increases rapidly

from  $0.459 \Omega$  ( $\sigma = 0$ ) to  $14.367 \Omega$  ( $\sigma = 0.89$ ).

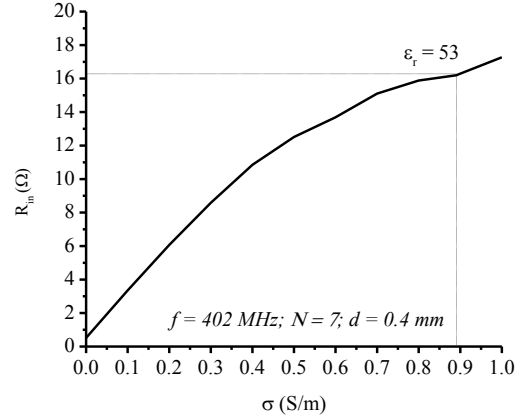


Fig. 7: Input Resistance of  $A_2$  structure depend on  $\sigma$

The effect of the conductivity ( $\sigma$ ) and material size ( $W$ ) on the input resistance ( $R_{in}$ ) is shown in  $A_2$  structure at Fig. 8. Solid lines illustrate simulation results with relative permittivity of  $\epsilon_r = 53$ . The input resistance  $R_{in}$  increases as conductivity of material increases. The input resistance  $R_{in}$  is obtained around  $20 \Omega$  with conductivity is  $\sigma = 0.8 \sim 1.1$  S/m and  $\sigma = 0.5 \sim 0.79$  S/m  $R_{in}$  is obtained around  $15 \Omega$ . With the conductivity of  $\sigma = 0.3 \sim 0.49$  S/m,  $R_{in}$  is obtained around  $10 \Omega$  and  $\sigma = 0 \sim 0.29$  S/m,  $R_{in}$  is obtained around  $5 \Omega$ . Input resistance  $R_{in}$  becomes smallest and it is obtained  $0.459 \Omega$  when  $\sigma = 0$  S/m. The conductivity of material mainly affects to the value of input resistance ( $R_{in}$ ). All of the cases, input resistance  $R_{in}$  does not depend on the material size ( $W$ ).

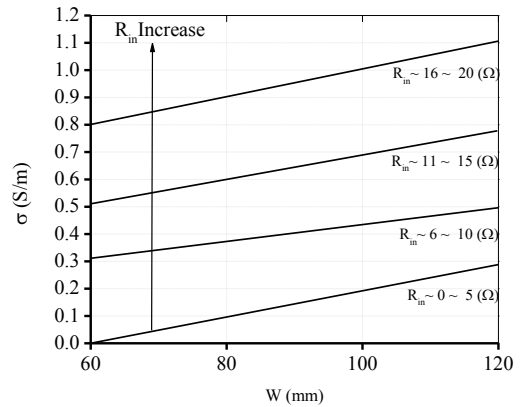


Fig. 8: Effect of  $\sigma$  and  $W$  to Input Resistances of  $A_2$  structure

## VI. RADIATED FIELDS

### A. Loss equation of human body

Human tissues consist of the great relative permittivity and conductivity. Therefore, human tissues have characteristics of

dielectric loss. In this case, wave propagation will be absorbed by human body. In order to estimate power degradation theoretically, propagation constants of a plane wave are examined [7]. Wave propagation model is shown in Fig. 9(a).

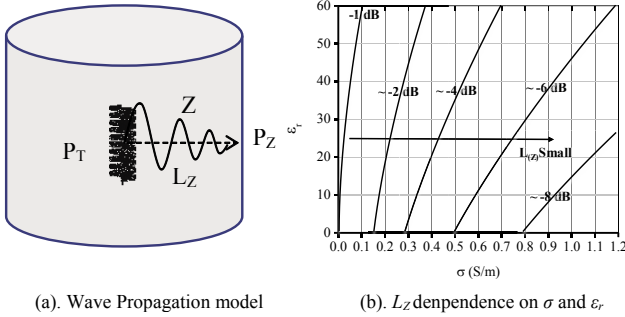


Fig. 9: Affect of  $\sigma$  and  $\epsilon_r$  to Propagation loss

In order to estimate loss propagation ( $L_Z$ ) of NMHA inside human body, the equation is presented as following:

$$L_Z = \frac{P_Z}{P_T} = \left| \frac{E_x(z)}{E_0} \right|^2 = e^{-2bz} \quad (5)$$

where,  $Z$  indicates distance from antenna to surface of material.  $P_T$  is transmitted power from antenna and  $P_Z$  is detected power in the surface of material.  $b$  indicates the power part of wave and is expressed as the following:

$$b = \sqrt{\frac{\omega^2 \epsilon \mu}{2}} \sqrt{\sqrt{1 + \frac{\sigma^2}{\omega^2 \epsilon^2}} - 1} \quad (6)$$

From Eq. (6), power loss by human tissues can be estimated and is fundamental for determining antenna gain. The calculation results of the propagation loss in the human body are shown in the Fig. 9(b). The propagation loss in the human body decreases as the conductivity of material increases. The propagation loss in the human body decreases as the relative permittivity of material decreases. Calculation results of loss propagation that investigated structure  $A_2$  are 0 dB and -5.7 dB corresponding to  $\sigma = 0$  S/m and  $\sigma = 0.89$  S/m.

### B. Calculated radiation pattern

The simulation results of NMHA's total gain in the human body are shown in Fig. 10. Radiation patterns of NMHA structures, that are investigated  $A_1, A_2, A_3$  in two case  $\sigma = 0$  S/m and  $\sigma = 0.89$  S/m are show in Fig. 10(a), 10(b) respectively. In calculation, "No mismatching mode" is selected. Then input powers are sufficiently transmitted to antenna. In  $\sigma = 0$  S/m, antenna gain become almost -8 dBi. In  $\sigma = 0.89$  S/m, antenna gain reduced to almost -28 dBi. In order to understand gain reductions by  $\sigma$  value, gain budget of TABLE III is obtained based on simulation results.

Theoretically, antenna efficiency ( $\eta$ ) and radiation resistances of equivalent small dipole ( $R_{rD}$ ) and small loop

TABLE III: GAIN REDUCTION BUDGET

	$\eta$ (dB)	$L_z$ (dB)	Gain (dBi)	$R_{in}$ ( $\Omega$ )	$R_r$ ( $\Omega$ )
$\sigma = 0$ (S/m)	-9.9	0	-8.2	0.46	0.046
$\sigma = 0.89$ (S/m)	-28.4	-5.7	-28.0	16.4	0.046

( $R_{rL}$ ) are given in Eq. (7) to (9), respectively. Antenna ohmic loss is given by Eq. (10). The  $R_r = R_{rD} + R_{rL}$  data in TABLE III is obtained by putting  $\eta = -9.9$  dB and  $R_{in} = 0.46 \Omega$  values to Eq. (7). Then, by using  $R_r = 0.046 \Omega$  and  $R_{in} = 16.4 \Omega$  at  $\sigma = 0.89$  S/m,  $\eta = -25.5$  dB is obtained. By taking the absorption of  $L_z = -5.7$  dB by  $\sigma = 0.89$  S/m material into account, radiation efficiency becomes  $\eta = -31.2$  dB. The efficiency of  $\eta = -28.4$  dB at TABLE III is about 3 dB larger than  $\eta = -31.2$  dB. This difference may be attributed to the accuracy of  $R_r$  value.

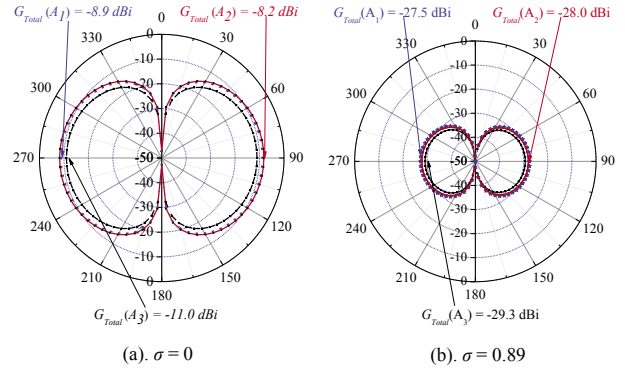


Fig. 10: Radiated pattern

$$\eta = \frac{R_{rD} + R_{rL}}{R_{in}}, \quad (7)$$

$$R_{rD} = \frac{20\pi^2}{\sqrt{\epsilon_r}} \left(\frac{H}{\lambda_g}\right)^2 \quad (8)$$

$$R_{rL} = 20\pi^6 \left(\frac{D}{\lambda_g}\right)^4 \left(\frac{N}{\sqrt{\epsilon_r}}\right) \quad (9)$$

$$R_{\Omega} = \frac{L_t}{d} \sqrt{\frac{120}{\sigma \lambda_g \sqrt{\epsilon_r}}} \quad (10)$$

## VII. CONCLUSION

Antenna design method and electrical characteristics of very small normal-mode helical antennas placed in a human body are clarified through electromagnetic simulations. Antenna sizes are 0.03 to 0.06 wave lengths in a human body condition. Self-resonant structures are clarified. Antenna input resistances are affected strongly by conductivity of a human body. Then, antenna efficiencies and gains are also affected by conductivity.

REFERENCES

- [1] A. C. Authority, "Planning for medical implant communications systems," *Proposals Paper*, vol. 1, no. 1, p. 18, 2003.
- [2] M. Appleyard, A. Glukhovskiy, and P. Swain, "Wireless-capsule diagnostic endoscopy for recurrent small-bowel bleeding," *New England Journal of Medicine*, vol. 344, no. 3, pp. 232–233, 2001.
- [3] ASGE, "Wireless capsule endoscopy," 2013.
- [4] "Feko suite 7," EM Software and Systems.
- [5] N. Q. Dinh, N. Michishita, Y. Yamada, and K. Nakatani, "Design Method of a Tap Feed for a Very Small Normal Mode Helical Antenna," *IEICE Transactions on Communications*, vol. J94-B, no. 2, pp. 164-175, Feb. 2011.
- [6] N. Q. Dinh, N. Michishita, Y. Yamada, and K. Nakatani, "Deterministic Equation for Self-Resonant Structures of Very Small Normal-Mode Helical Antennas," *IEICE Transactions on Communications*, vol. E94-B, no. 5, pp. 1276-1279, May 2011.
- [7] J. William Hayt, "Wave propagation in dielectrics," *Engineering Electromagnetics*, vol. Eighth Edition, pp. 376–379, 2012.
- [8] N. T. Tuan, Y. Yamada, N. Q. Dinh, and N. Michishita, "Self-resonant structures of normal-mode helical antennas embedded in dielectric and magnetic materials," *Proceedings of the Advanced Technologies for Communications*, pp. 627–632, 2015.
- [9] D. T. Dung, N. Q. Dinh, N. T. Tuan, Y. Yamada, and N. Michishita, "Simulation Methods of a Normal-Mode Helical Antenna in a Human Body Condition," *Proceedings of the Advanced Technologies for Communications*, pp. 380-383, 2016.